

Controlling dopant profiles in hyperdoped silicon by modifying dopant evaporation rates during pulsed laser melting

Daniel Recht,¹ Joseph T. Sullivan,² Robert Reedy,³ Tonio Buonassisi,² and Michael J. Aziz^{1,a)}

¹Harvard School of Engineering and Applied Sciences, Cambridge, Massachusetts 02138, USA

²Department of Mechanical Engineering, Massachusetts Institute of Technology, Cambridge, Massachusetts 02139, USA

³National Renewable Energy Laboratory, Golden, Colorado 80401, USA

(Received 2 February 2012; accepted 1 March 2012; published online 16 March 2012)

We describe a method to control the sub-surface dopant profile in “hyperdoped” silicon fabricated by ion implantation and pulsed laser melting. Dipping silicon ion implanted with sulfur into hydrofluoric acid prior to nanosecond pulsed laser melting leads to a tenfold increase in the rate of sulfur evaporation from the surface of the melt. This results in an 80% reduction of the near-surface dopant concentration, effectively embedding the hyperdoped region in a layer up to 180 nm beneath the surface. This method should facilitate the development of blocked impurity band devices. © 2012 American Institute of Physics. [<http://dx.doi.org/10.1063/1.3695171>]

Silicon (Si) doped to roughly 1 at. % (i.e., hyperdoped) with chalcogens by ion implantation and nanosecond pulsed laser melting (PLM) has attracted interest as a potential material for intermediate band (IB) photovoltaics and advanced light detectors because of its broad optical absorption beyond the band gap of silicon.^{1–3} An important aspect of many intermediate band devices is the need to “block” the IB from the charge collecting electrodes to ensure that the operating voltage is determined by the largest energy gap of the IB material. This can be accomplished by sandwiching the IB layer between a pn-junction and a lightly doped blocking layer, but requires that the heavily doped layer begin some distance below the device’s surface.⁴ Although ion implantation and PLM can produce single-crystal silicon with the requisite high doping levels, they have never been used to form buried hyperdoped layers. In this letter, we report a method for creating these previously inaccessible structures.

Models of laser melting and rapid resolidification, and of dopant diffusion/evaporation in the melt have been developed that can accurately predict the post-solidification dopant profile based on the as-implanted dopant profile.^{3,5,6} These models have revealed that surface evaporation of high vapor pressure dopants such as sulfur (S) and nitrogen can be significant during pulsed laser melting of semiconductors.^{3,5} While silicon is known⁷ to retain its native oxide during nanosecond laser melting, the effect of the native oxide on dopant evaporation has never been probed. Here, we demonstrate that removing the surface oxide prior to PLM significantly increases the surface evaporation rate of S from the melt and allows the formation of a buried hyperdoped layer.

750 μm thick double-side polished p-type Si(001) wafers with resistivity 10–30 $\Omega\text{ cm}$ were ion implanted at room temperature with 95 keV $^{32}\text{S}^+$ to a dose of 1×10^{16} ions/cm². Ion-implanted samples were then irradiated with one or four pulses from a spatially homogenized, pulsed XeCl⁺ excimer

laser (308 nm, 25 ns full width at half maximum, 50 ns pulse duration) with a square spot approximately $3 \times 3\text{ mm}^2$. A fluence of 1.7 J/cm^2 was used for the one-pulse samples and for the first three shots on the four-pulse samples. 1.8 J/cm^2 was used for the fourth shot to ensure that the final melt was the deepest; this prevented exposure of supersaturated material produced in previous shots to non-melting thermal treatment. Laser fluences were calibrated by comparing the measured melt duration of an untreated Si wafer with numerical solutions to the one-dimensional heat equation.^{8,9} Melt duration was monitored *in-situ* via time-resolved reflectivity using a low-power 488 nm Ar⁺ ion laser. Laser melting and the subsequent rapid solidification form a single-crystal region that retains most of the implanted impurities but that is free of extended defects.^{10,11} This region has the lateral extent of the laser spot and a thickness corresponding to the melt depth ($\sim 350\text{ nm}$).

To test the effects of the native oxide on surface evaporation, some samples were oxide-etched in 10% hydrofluoric acid for 30 s to remove the native oxide within 4 h before PLM. The time between etching and melting was short enough that we would expect the etched samples to have an oxide that is less than half the thickness ($\sim 0.2\text{ nm}$) of that on the un-etched samples ($\sim 1\text{ nm}$).¹² In addition, samples were melted in a variety of atmospheres: air, flowing argon, and a chamber evacuated and then back-filled with argon. S concentration depth profiles of as-implanted and laser melted samples were measured by dynamic secondary ion mass spectrometry (SIMS) using a Cameca IMS-5F instrument with a Cs⁺ primary beam.

The final S concentration profiles (as measured by SIMS) of samples melted in the three atmospheres tested here were not noticeably different. Thus, the remainder of this letter will focus on the effects of etching away the native oxide. Figure 1 plots the S concentration profiles of as-implanted material and of an etched sample melted with a single laser shot. Points within 10 nm of the surface are included for completeness, but are of substantially higher

^{a)}Author to whom correspondence should be addressed. Electronic mail: aziz@seas.harvard.edu.

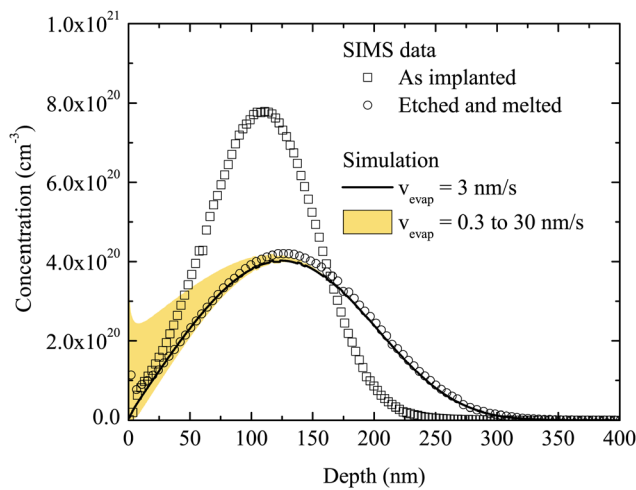


FIG. 1. (Color online) Sulfur concentration depth profiles obtained by SIMS for a sample treated with HF to remove the native oxide and then melted with a single laser shot. The simulations shown use the best-fit values of the diffusivity of S in liquid Si ($2.7 \times 10^{-4} \text{ cm}^2/\text{s}$) and diffusive velocity (1.0 m/s). The shaded region shows the sensitivity of the simulation to changes in the surface evaporation velocity. For the lower concentration limit, the surface evaporation velocity is an order of magnitude greater, and for the upper concentration limit an order of magnitude lower, than the best-fit value of 3.0 nm/s. The surface evaporation velocity of 0.3 nm/s, which leads to the upper concentration limit, is the value obtained previously³ for a sample with a mature native oxide but otherwise nominally identical to this one.

uncertainty because they were collected before steady-state sputtering conditions were reached during the SIMS measurement. Aside from oxide removal, the melted sample received the same treatment as those measured in Ref. 3. Nevertheless, it is clear from Figure 1 that the surface concentration of S in the sample that underwent oxide removal is well below the $2 \times 10^{20} \text{ cm}^{-3}$ reported in that paper (cf. their Figure 2).³ Figure 1 also shows the results of simulations of the laser melting and S diffusion/evaporation processes. The best fit values (as determined by visual inspection) of the diffusivity, diffusive velocity, and surface evaporation velocity (analogous to the surface recombination

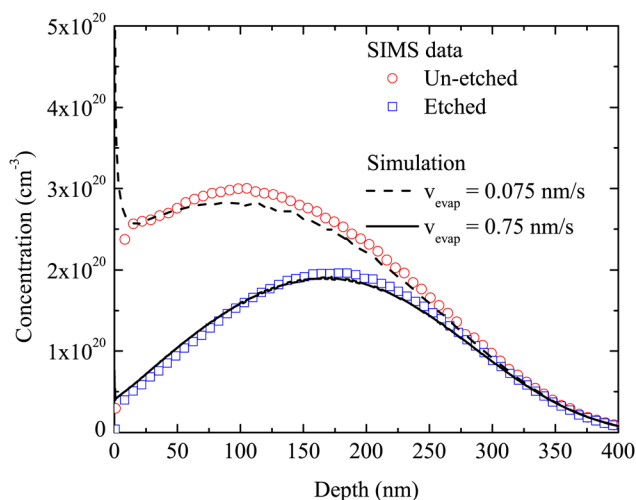


FIG. 2. (Color online) Sulfur concentration depth profiles and simulations for etched and un-etched samples melted four times by consecutive laser shots. The simulations shown use the best-fit values of the diffusivity of S in liquid Si ($2.7 \times 10^{-4} \text{ cm}^2/\text{s}$) and diffusive velocity (1.0 m/s). A constant surface evaporation velocity was assumed for all four melting events.

velocity of charge carriers) are $2.7 \times 10^{-4} \text{ cm}^{-2}$, 1 m/s, and 3 nm/s, respectively. The diffusivity and diffusive velocity fits were performed over all samples, while the surface evaporation velocity fits were performed separately for the 1-shot and 4-shot samples. While the discrepancy in diffusivity between our result and the value of $1.4 \times 10^{-4} \text{ cm}^{-2}$ reported in Ref. 3 could conceivably be due to differences in the ion implanters used, it is most likely the result of measurement uncertainty. This uncertainty could exist either in the depth calibration of SIMS data by measuring the final crater depth with stylus profilometry or in the peak concentration because of the correction¹³ for secondary ion counter dead-time (i.e., detector saturation) in the measurements reported in Ref. 3.

The shaded region in Figure 1 indicates the sensitivity of the simulated concentration profiles to different values of the surface evaporation velocity. As can be seen from the figure, faster evaporation velocities lead to relatively small deviations toward lower surface concentration from the best-fit profile because the best-fit velocity is fast enough to reduce the surface S concentration to nearly nil. Slower evaporation velocities, however, lead to large deviations toward higher surface concentrations. A surface evaporation velocity of 0.3 nm/s (comparable to the value of 0.27 nm/s of Ref. 3) yields a predicted surface concentration far greater than what is observed. This indicates that etching the surface oxide yields a tenfold increase in the rate of surface evaporation relative to an un-etched sample.

Figure 2 compares data and simulations of the sulfur concentration profiles of samples pulsed laser melted four times with and without oxide removal. Etching the surface oxide leads to an order-of-magnitude decrease in the surface S concentration and shifts the peak S concentration deeper by more than 50 nm. The sample whose oxide was removed thus possesses a buried layer of hyperdoped silicon produced by ion implantation and pulsed laser melting. The best fit surface evaporation velocity (assuming, for simplicity, the same value for all four melting events) for the etched and un-etched samples is 0.75 nm/s and 0.075 nm/s, respectively, once again demonstrating a tenfold increase in the evaporation rate due to removal of the native oxide. The value for the sample whose native oxide remained intact is consistent within experimental error with the value of 0.054 nm/s ³ of Ref. 3. Comparing this to the value for the one-shot sample discussed above suggests that the surface evaporation velocity decreases with successive laser shots, possibly because of the growth of additional native oxide at the elevated surface temperatures present for a few hundred nanoseconds after melting. A similar decrease in evaporation velocity between one- and four-shot samples was reported previously.³

The technological implications of control over the surface evaporation rate are numerous. Figures 1 and 2 indicate that the surface S concentration can be lowered to such an extent that counter-doping with boron,¹⁴ for example, could easily yield a fully compensated or p-type surface with a buried hyperdoped layer similar to that used in the first impurity band photovoltaic cell.⁴ Furthermore, because of the ease with which silicon's surface oxide may be laterally patterned, modulating surface evaporation represents a straightforward route to lateral control of the S doping profile.

We have demonstrated that etching silicon's native oxide increases tenfold the surface evaporation rate of sulfur during nanosecond pulsed laser melting. This simple method for controlling surface evaporation greatly broadens the range of doping profiles and devices that can be fabricated using sulfur ion implantation and pulsed laser melting. As a demonstration, we have used this phenomenon to produce a buried layer of silicon hyperdoped with sulfur.

D.R. and M.J.A. were supported by a grant from the U.S. Army-ARDEC under Contract No. W15QKN-07-P-0092. J.T.S. acknowledges a National Science Foundation Graduate Research Fellowship. J.T.S. and T.B. acknowledge support from the U.S. Army Research Laboratory and the U.S. Army Research Office under grant no. W911NF-10-1-0442; and the National Science Foundation under contract no. ECCS-1102050. The Center for Nanoscale Systems (CNS) is supported by NSF award no. ECS-0335765. We thank Sally Asher for enabling the collaboration with NREL and for scientific discussions.

- ¹S. H. Pan, D. Recht, S. Charnvanichborikarn, J. S. Williams, and M. J. Aziz, *Appl. Phys. Lett.* **98**, 121913 (2011).
- ²A. J. Said, D. Recht, J. T. Sullivan, J. M. Warrender, T. Buonassisi, P. D. Persans, and M. J. Aziz, *Appl. Phys. Lett.* **99**, 073503 (2011).
- ³B. P. Bob, A. Kohno, S. Charnvanichborikarn, J. M. Warrender, I. Umezu, M. Tabbal, J. S. Williams, and M. J. Aziz, *J. Appl. Phys.* **107**, 123506 (2010).
- ⁴N. López, L. Reichertz, K. Yu, K. Campman, and W. Walukiewicz, *Phys. Rev. Lett.* **106**, 28701 (2011).
- ⁵T. Kim, K. Alberi, O. D. Dubon, M. J. Aziz, and V. Narayanamurti, *J. Appl. Phys.* **104**, 113722 (2008).
- ⁶T. Kim, M. R. Pillai, M. J. Aziz, M. A. Scarpulla, O. D. Dubon, K. M. Yu, J. W. Beeman, and M. C. Ridgway, *J. Appl. Phys.* **108**, 013508 (2010).
- ⁷G. Jellison and D. Lowndes, *Appl. Phys. Lett.* **51**, 352 (1987).
- ⁸R. Reitano, P. M. Smith, and M. J. Aziz, *J. Appl. Phys.* **76**, 1518 (1994).
- ⁹M. J. Aziz, *Metall. Mater. Trans. A* **27**, 671 (1996).
- ¹⁰R. Young, J. Narayan, and R. Wood, *Appl. Phys. Lett.* **35**, 447 (1979).
- ¹¹M. Tabbal, T. Kim, J. M. Warrender, M. J. Aziz, B. Cardozo, and R. Goldman, *J. Vac. Sci. Technol. B* **25**, 1847 (2007).
- ¹²M. Morita, T. Ohmi, E. Hasegawa, M. Kawakami, and M. Ohwada, *J. Appl. Phys.* **68**, 1272 (1990).
- ¹³B. Bob, lab notebook, unpublished notes.
- ¹⁴K. Sánchez, I. Aguilera, P. Palacios, and P. Wahnón, *Phys. Rev. B* **82**, 165201 (2010).